NANO LETTERS

pubs.acs.org/NanoLett

Transformation Optics for Plasmonics

Paloma A. Huidobro,[†] Maxim L. Nesterov,[†,‡] Luis Martín-Moreno,[§] and Francisco J. García-Vidal*[,†]

[†]Departamento de Física Teórica de la Materia Condensada, Universidad Autónoma de Madrid, E-28049 Madrid, Spain, [‡]A. Ya. Usikov Institute for Radiophysics and Electronics, NAS of Ukraine, 12 Academician Proskura Street, 61085 Kharkov, Ukraine, and [§]Instituto de Ciencia de Materiales de Aragón and Departamento de Física de la Materia Condensada, CSIC-Universidad de Zaragoza, E-50009 Zaragoza, Spain

ABSTRACT A new strategy to control the flow of surface plasmon polaritons at metallic surfaces is presented. It is based on the application of the concept of transformation optics to devise the optical parameters of the dielectric medium placed on top of the metal surface. We describe the general methodology for the design of transformation optical devices for surface plasmons and analyze, for proof-of-principle purposes, three representative examples with different functionalities: a beam shifter, a cylindrical cloak, and a ground-plane cloak.

KEYWORDS Surface plasmons, transformation optics, metamaterials

Transformation optics (TO) has been proposed[1,2] as a general technique to design complex electromagnetic (EM) medium with unusual properties. In order to construct novel optical devices, one has to imagine a space with some distortion in a certain region and make a coordinate transformation from a flat empty space. Due to the form invariance of Maxwell equations under general coordinate transformations,[3] the properties of the distorted geometry can then be interpreted as that of a medium in the original flat empty space.[4] Thus, TO provides us with expressions for the dielectric permittivity tensor, $\hat{\varepsilon}$, and the magnetic permeability tensor, $\hat{\mu}$, that need to be implemented in order to obtain a medium with a designed functionality. The first practical realization of this idea was the construction of a two-dimensional (2D) cylindrical invisibility cloak for EM waves in the microwave regime.[5] This experiment took advantage of the recently developed field of metamaterials.[6,7] These are artificially structured materials made up of subwavelength constituents and designed to implement a prescribed response to EM fields. The cylindrical cloak experiment was followed by the construction of broad-band cloaks in the microwave[8] and optical[9,10] regimes, all of them based on a different strategy, the so-called ground-plane cloak.[11] Besides, a wide variety of applications other than cloaking has been recently presented, including beam shifters and beam dividers,[12] field concentrators,[13] collimators,[14] waveguide bends and corners,[15] lenses with subwavelength resolution,[16] or deep-subwavelength waveguides.[17]

In plasmonics, one of the main goals is to control the flow of light at a metal surface by means of the surface plasmon polaritons (SPPs) that decorate a metal−dielectric interface.[18,19] In the quest for creating photonic circuits based on SPPs, different waveguiding schemes have been tested during the last years (see, for example, the recent review articles[20,21]). At a different level, 2D optical elements for SPPs like mirrors and beam splitters based on Bragg-scattering of SPPs with periodic arrays of scatterers have been also devised.[22]

In this paper we present a different strategy to tackle this problem by showing how the TO framework can be applied to mold the propagation of SPPs at a metal surface. As TO is valid for any source of illumination due to the universal character of Maxwell equations, it is expected that TO recipes will be also operative for SPPs. These EM modes are surface waves traveling along the interface between two media, a dielectric and a metal. Therefore, in order to design an optical device for SPPs, the expressions for the EM material parameters provided by the TO formalism should, in principle, be implemented both in the dielectric and the metal sides. This fact is a severe technical challenge, as TO generally requires highly anisotropic and inhomogeneous $\hat{\varepsilon}$ and $\hat{\mu}$. Moreover, the decay length of the SPP within the metal, i.e., the skin depth, is subwavelength, which means that a manipulation of $\hat{\varepsilon}$ and $\hat{\mu}$ at a nanometer scale within the metal would be needed. However, we will show in the following that a simplified version of the TO recipe in which only the dielectric side is manipulated leads to quasi-perfect functionalities. Two factors determine whether this simplification is operative or not: the wavelength of the SPP and the geometry of the device under consideration. In order to illustrate this point, we discuss here three very different devices: a beam shifter, a cylindrical cloak and a ground-plane cloak for SPPs.

As a first illustration of our methodology, we consider the 3D implementation for SPPs of a parallel beam shifter recently proposed by Rahm and co-workers for 2D geom-

* To whom correspondence should be addressed, fj.garcia@uam.es.
Received for review: 03/5/2010
Published on Web: 05/13/2010

DOI: 10.1021/nl100800c | *Nano Lett.* **2010,** *10,* 1985–1990

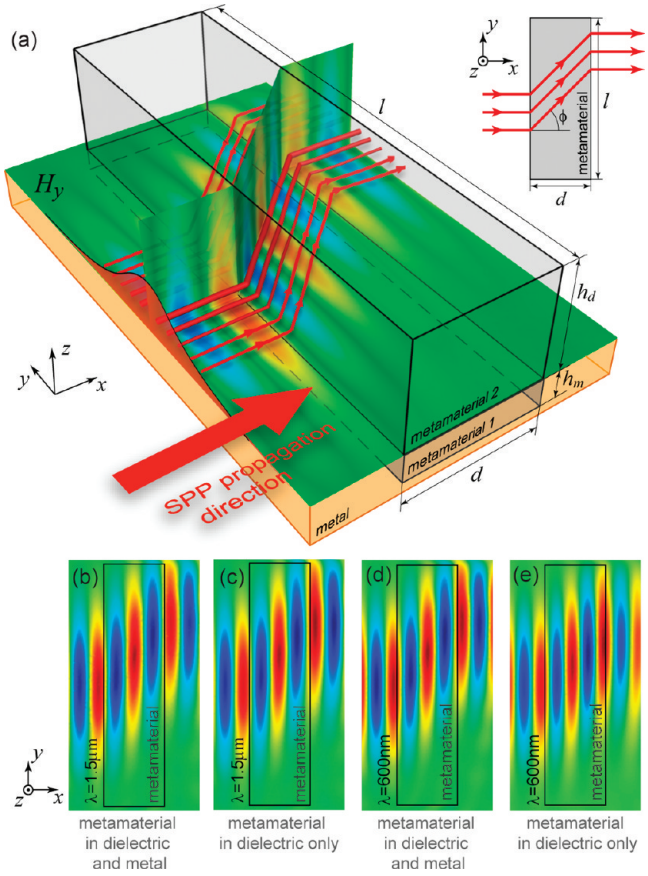

FIGURE 1. Normalized magnetic field pattern (color map) of a SPP traveling along a gold−vacuum interface and entering into a 3D beam shifter. Inset of panel a shows the basic geometry of the 2D case. Panel a depicts a 3D view with power flow streamlines of a SPP operating at $\lambda = 1.5$ μm. The prescribed $\hat{\varepsilon}$ and $\hat{\mu}$ were implemented in two rectangular parallelepipeds with in-plane dimensions 2.5 μm × 10 μm and thicknesses $h_d = 6$ μm and $h_m = 50$ nm. Panel b renders a cross-section picture of panel a evaluated at the metal surface, $z = 0$. For comparison, panel c shows a SPP beam shifter where the slab with the prescribed $\hat{\varepsilon}$ and $\hat{\mu}$ has been introduced only in the dielectric side. Panels d and e render the operation of a beam shifter for a SPP of $\lambda = 600$ nm. In this case the in-plane dimensions of the rectangular slabs are 1 μm × 4 μm and the thicknesses are $h_d = 600$ nm and $h_m = 50$ nm. In panel e, only the dielectric side is manipulated.

etry.[12] Let us discuss first this 2D case that was the first report of a finite embedded transformation, which is capable of transferring the modification of the EM fields to the wave that exits the TO medium. In the design of the 2D beam shifter, a rectangular region of sides d and l is considered and a transformation is performed from a 2D Cartesian grid into a grid that is tilted at an angle ϕ (see inset of Figure 1a). The amount of shift that the incident beam will experience is given by $a = \tan \phi$, which we will set to 1 ($\phi = 45°$) throughout this work for simplicity. The symmetry of the 2D problem for a EM plane wave implies that the two polarizations can be treated separately. For a wave polarized with the electric field perpendicular to the plane of the transformation, a TM plane wave, the relevant EM parameters obtained for the transformation medium according to TO are $\varepsilon_{zz} = 1$, $\mu_{xx} = 1$, $\mu_{xy} = \mu_{yx} = a$, and $\mu_{yy} = 1 + a^2$.

To design a 3D beam shifter for a SPP propagating along the interface between a metal and a dielectric, we perform the embedded transformation in parallelepipeds of rectangular base ($d \times l$). Two different transformation media are needed, one in the dielectric, with height h_d, and one in the metal (height h_m). Notice that in order to operate over the entire SPP field, the height of the rectangular slab in each medium must be greater than the corresponding decay length of the SPP in that medium (metal or dielectric). The expressions for $\hat{\varepsilon}$ and $\hat{\mu}$ inside the dielectric slab in a Cartesian basis are independent of the z coordinate and are

$$\hat{\varepsilon}_{TO} = \hat{\mu}_{TO} = \begin{pmatrix} 1 & a & 0 \\ a & 1 + a^2 & 0 \\ 0 & 0 & 1 \end{pmatrix} \quad (1)$$

where we have assumed that the dielectric half-space is vacuum without any loss of generality. On the other hand, the two tensors in the metallic slab should be

$$\hat{\varepsilon} = \hat{\varepsilon}_{TO} \cdot \varepsilon_m, \quad \hat{\mu} = \hat{\mu}_{TO} \quad (2)$$

where ε_m is the electric permittivity of the metal.

To test the TO recipe for a SPP beam shifter, we have carried out 3D full-wave simulations using the COMSOL Multiphysics software that is based on the finite element method (FEM). Figure 1a shows a 3D view of the behavior of a SPP at $\lambda = 1.5$ μm going through a beam shifter. The incident SPP, which displays a Gaussian profile in the y direction, propagates along the x direction through a gold−vacuum interface and enters into the transformation medium, where it is shifted in the y direction. Details on the geometrical parameters can be found in the caption of Figure 1. In this simulation, rectangular slabs with the prescribed $\hat{\varepsilon}$ and $\hat{\mu}$ were introduced in both the dielectric and metal sides. A cross section showing the behavior of H_y at the metal surface ($z = 0$) is rendered in Figure 1b. Parts b and c of Figure 1 allow us to compare the quality of the shift whether we implement $\hat{\varepsilon}$ and $\hat{\mu}$ in the dielectric and metal sides (b) or only in the dielectric side (c). It is worth noticing that there is almost no difference between the field distributions in both cases. On the other hand, parts d and e of Figure 1 show the corresponding cross sections at $z = 0$ of the beam shifter for a SPP but now operating at $\lambda = 600$ nm for the case of placing the transformation media in the dielectric and metal sides (d) and when only the dielectric side is manipulated (e). Although the effectiveness of the shifter at this wavelength is affected by the absence of a transformation medium in the metal side, its functionality (a shift in the SPP beam) is still very good. The reason for this weak

DOI: 10.1021/nl100800c | *Nano Lett.* **2010,** *10,* 1985–1990

wavelength dependence is clear. The vacuum decay length of a SPP on a gold surface at 1.5 μm is 2.4 μm, much larger than the skin depth (23 nm) so the EM fields within the metal carry 0.01 % of the total SPP energy, having practically no relevance compared to the EM fields in the dielectric. However, at $\lambda = 600$ nm, the ratio between vacuum decay length of the SPP and skin depth is reduced by a factor of 10 and the EM fields inside the metal are then relatively more important for the propagation of the SPP. For this wavelength, 1 % of the SPP energy resides in the metal.

As a second example, we present a 3D cylindrical cloak for SPPs based on TO. Here we aim for suppressing the scattering of a SPP from an object placed on a surface and not to use plasmonic structures to achieve cloaking.[23] Note that other strategies for SPP cloaking that do not rely on the TO framework have been recently proposed.[24] As stated above, the 2D invisibility cloak was the first application of TO, both in theoretical proposals[1,2] and in experiments.[5] The design of a 3D cylindrical cloak for SPPs is analogous to that of the beam shifter. The field distribution of the SPP extends itself in the dielectric and in the metal, so, in principle, we should again cloak the SPP-field in both regions of space. Because of the presence of the metal−dielectric interface, we apply the 2D cylindrical transformation as described by Pendry and co-workers[1] in planes that are parallel to the interface, building-up two concentric cylinders of radii a and b (see Figure 2a). In each plane, we perform a transformation from flat 2D Euclidean space, where light propagates in straight lines, to a space with a hole of radius a surrounded by a compressed region of radius b. The transformation medium is the shell comprised between a and b and is expected to guide the incident SPP around the hole. The SPP wave will emerge at the other side as if it had traveled through an empty space. The $\hat{\varepsilon}$ and $\hat{\mu}$ tensors obtained for the transformation medium in the dielectric half-space read as follows in a cylindrical basis

$$\hat{\varepsilon}_{\mathrm{TO}} = \hat{\mu}_{\mathrm{TO}} = \begin{pmatrix} \dfrac{r-a}{r} & 0 & 0 \\ 0 & \dfrac{r}{r-a} & 0 \\ 0 & 0 & \left(\dfrac{b}{b-a}\right)^2 \dfrac{r-a}{r} \end{pmatrix} \quad (3)$$

Cloaking the SPP field inside the metal would require a cylindrical transformation medium whose magnetic permeability is the same as in the dielectric side, $\hat{\mu}_{\mathrm{TO}}$, while its electric permittivity is simply $\hat{\varepsilon}_{\mathrm{TO}} \cdot \varepsilon_{\mathrm{m}}$.

3D simulations of the cylindrical cloak for SPPs operating at $\lambda = 1.5$ μm (panels b and c) and $\lambda = 600$ nm (panels d and e) are shown in Figure 2. In these cases, the prescribed $\hat{\varepsilon}$ and $\hat{\mu}$ were implemented only in the dielectric, in a cylindrical shell surrounding a perfectly conducting cylinder, leaving the metal as a continuous sheet. We present for each

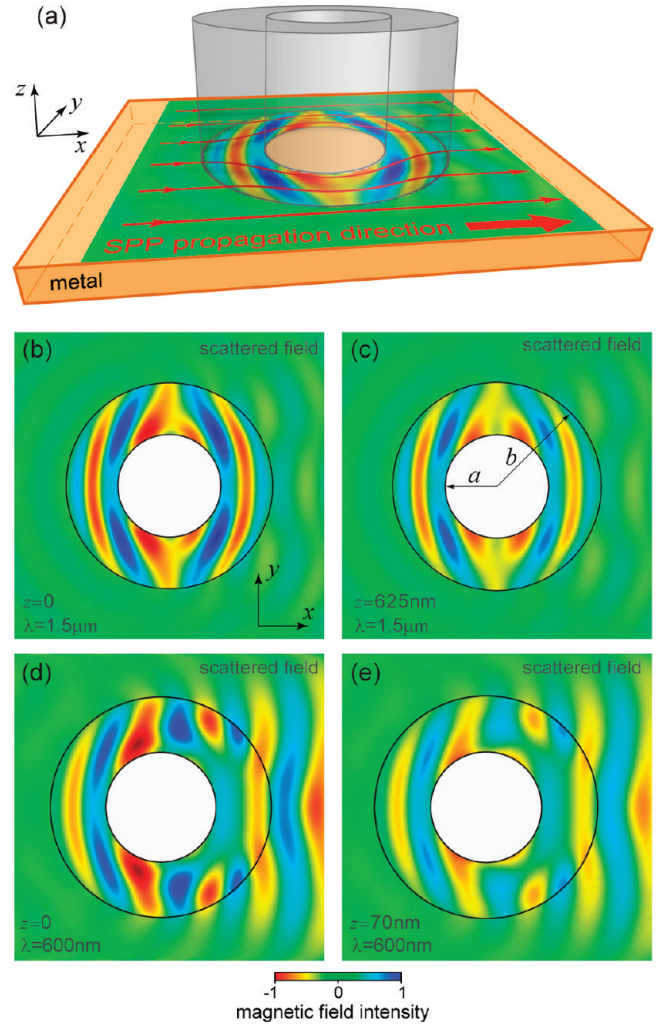

FIGURE 2. Scattered magnetic field for a 3D cylindrical cloak for SPPs. (a) A schematic picture showing the geometry of the cloak. Cloaking parameters are implemented only in the dielectric side, in the region between the inner radius a and the outer radius $b = 2a$. The operating wavelength is 1.5 μm in panels b and c and the cylindrical cloak in this case is 6 μm high with $a = 1.5$ μm. (b) Scattered H_y field evaluated at the metal surface, $z = 0$. (c) The corresponding field as obtained at $z = 625$ nm, a quarter of the vacuum decay length of the SPP into the dielectric. In panels d and e the wavelength is 600 nm and the cloak is 600 nm high with $a = 500$ nm. (d) Scattered H_y field obtained at $z = 0$ plane. (d) The same quantity but now evaluated at $z = 70$ nm, a quarter of the vacuum decay length of the SPP for $\lambda = 600$ nm.

wavelength the y component of the scattered magnetic field evaluated at two planes parallel to the metal−dielectric interface, one at $z = 0$ (panels b and d) and another at a height at which the SPP has decayed to a quarter of its intensity at the interface (panels c and e). At $\lambda = 1.5$ μm, the scattered magnetic field is nearly zero out of the cloaking region and we can conclude that the performance of the cloaking device for SPPs is excellent. However, for a SPP at a wavelength of 600 nm, only partial cloaking is achieved. The reason for this is the geometry of the cylindrical cloak which, as opposed to the beam shifter, has a discontinuity in the metal−dielectric interface. In this case, the behavior

DOI: 10.1021/nl100800c | *Nano Lett.* **2010,** *10,* 1985–1990

of the cloak is very sensitive to the field propagating inside the metal because it strongly scatters at this discontinuity. Simulations in which the metal is also manipulated according to the TO recipe were carried out (not shown here). In this case, the 3D cylindrical cloak for SPPs displays a perfect performance at the two wavelengths considered. Our results explain why a previous experiment on SPP cloaking at $\lambda =$ 500 nm in which the metamaterial was only placed in the dielectric side was not completely successful.[25]

Finally, we consider a different strategy for cloaking,[11] based on the use of TO to design a cloak that mimics a ground-plane (flat metal surface). We will show that in this case the simplification of using the transformation media only in the dielectric side works perfectly. The main difference between a ground-plane cloak and the rest of the TO-based devices that we have considered up to here is the geometry. A ground-plane cloak inherently needs to be placed on a metal surface, because it mimics a highly reflective surface instead of an empty space. Taking advantage of the presence of this metal−dielectric interface, we apply directly the TO recipe previously derived for a 2D ground-plane cloak illuminated by a plane wave[11] to the case of SPP illumination.

The design of a 2D ground-plane cloak[11] starts by considering a rectangular region of a flat space. The size of the rectangle is $l \times h$ and it sits on a metal surface. Suppose that we want to cloak a bump of maximum height h_0 and with a shape that follows the equation $z(x) = h_0 \cos^2(\pi x/l)$. Then we make a transformation from the rectangle to a region of the same shape except for its bottom boundary which is lifted following the surface of the bump. The simplest transformation consists of a transfinite mapping, which is not conformal.[26] This means that it does not preserve angles and hence the anisotropy is not minimized.[11] However, we will use it as a proof-of-concept of the performance of a ground-plane cloak for SPPs. If we place the cloak in the $x-z$ plane (see Figure 3), the EM fields along the y axis being translationally invariant, the transformation in a Cartesian basis reads

$$x = x',\ y = y',\ z = z' + h_0\left(1 - \frac{z'}{h}\right)\cos^2\left(\frac{\pi}{l}x'\right) \quad (4)$$

The optical parameters, $\hat{\varepsilon}$ and $\hat{\mu}$, for the transformation medium are obtained using the standard TO techniques

$$\hat{\varepsilon} = \hat{\mu} = \frac{1}{\Delta}\begin{pmatrix} 1 & 0 & f_{xz} \\ 0 & 1 & 0 \\ f_{xz} & 0 & f_{zz} \end{pmatrix} \quad (5)$$

where $\Delta = \partial z/\partial z'$, $f_{xz} = \partial z/\partial x'$, and $f_{zz} = f_{xz}^2 + \Delta^2$. The 2D ground-plane cloak for SPPs consists of a dielectric with the prescribed $\hat{\varepsilon}$ and $\hat{\mu}$ placed on a metal surface with a $\cos^2$ shaped bump. A SPP propagating along the metal−dielectric interface and entering into the ground-plane cloak should be smoothly guided around the bump. Figure 3a shows the magnetic field distribution of a SPP at $\lambda = 600$ nm traveling along a gold−vacuum interface and going through the cloak. Although only the dielectric medium is transformed in this 2D simulation, the SPP nicely follows the curvature of the bump at the two sides of the interface.

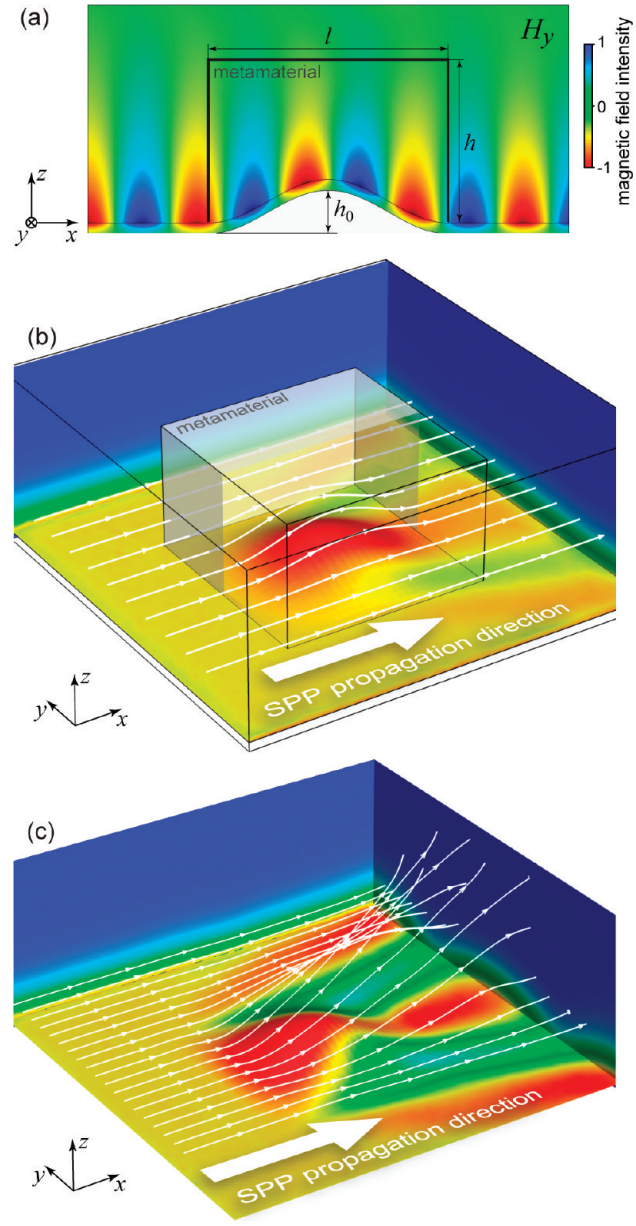

FIGURE 3. (a) Normalized magnetic field pattern of a 2D ground-plane cloak for a SPP traveling in the x direction at 600 nm. The cloaked object is a $\cos^2$ shaped gold bump, 1250 nm long and with a height of $h_0 = 200$ nm. The height of the cloak is $h = 750$ nm. (b) Power flow distribution (color map) and streamlines of a 3D ground-plane cloak placed over a 3D $\cos^2$ shaped gold bump of dimensions 1250 nm ×1250 nm ×200 nm. (c) Power flow for the 3D gold scatterer without the cloak.

A ground-plane cloak for SPPs can be also devised for hiding a 3D bump. In this case, the bump sits on the $x-y$

DOI: 10.1021/nl100800c | *Nano Lett.* **2010,** *10,* 1985–1990

plane and its surface is given by $z(x, y) = h_0 \cos^2(\pi x/l) \cos^2(\pi y/l)$. As for the 2D cloak, we make a transfinite transformation from a rectangular prism to a prism whose bottom boundary is lifted by the bump. In this case, the mathematical formulas for the transformation are

$$x = x',\ y = y',\ z = z' + h_0\left(1 - \frac{z'}{h}\right)\cos^2\left(\frac{2\pi}{l}x'\right)\cos^2\left(\frac{2\pi}{l}y'\right) \quad (6)$$

According to the TO rules, we obtain the $\hat{\varepsilon}$ and $\hat{\mu}$ for the transformation medium

$$\hat{\varepsilon} = \hat{\mu} = \frac{1}{\Delta}\begin{pmatrix} 1 & 0 & f_{xz} \\ 0 & 1 & f_{yz} \\ f_{xz} & f_{yz} & f_{zz} \end{pmatrix} \quad (7)$$

where $\Delta = \partial z/\partial z'$, $f_{xz} = \partial z/\partial x'$, $f_{yz} = \partial z/\partial y'$, and $f_{zz} = f_{xz}^2 + f_{yz}^2 + \Delta^2$. We present in Figure 3b a simulation that confirms the effectiveness of the 3D cloak for a SPP operating at $\lambda =$ 600 nm. The color map and the streamlines represent the density and the direction of the power flow of the SPP, respectively. The SPP is guided around the bump and continues traveling along the gold−vacuum interface. For comparison, Figure 3c shows a SPP scattering from the gold bump when the cloak is not present. We see that the fraction of the SPP that impinges directly into the bump is scattered upwards. This radiation into free space is totally suppressed when the cloak is present, as shown in Figure 3b.

Now we briefly discuss the practical realization of the TO-based devices for SPPs presented in this work. Our results have shown that the effectiveness of these devices is basically governed by the presence of a transformation medium in the dielectric side whereas modifying the metal side is not necessary in most of the cases. Then it is enough to realize anisotropic $\hat{\varepsilon}$ and $\hat{\mu}$ within the dielectric, making use of a specific metamaterial. Different tools for overcoming the necessity of anisotropic parameters have already been developed within the field of metamaterials. For instance, in the reduced parameters approach, the tensors are simplified so that only some components need to be implemented. This allows the design of nonmagnetic metamaterials operating in the optical regime,[27] a fact that has been applied to the construction of the 2D cylindrical cloak. On the other hand, isotropic $\hat{\varepsilon}$ and $\hat{\mu}$ are obtained when a conformal transformation[2] is performed, so it is enough to implement an isotropic refractive index. Numerical techniques have been recently developed to compute quasi-conformal coordinate transformations, which minimize anisotropy to a point where it is negligible.[11] In particular, the quasi-conformal mapping technique has proved useful for the practical realization of the 2D ground-plane cloak for plane wave illumination[9] or for building-up a curved reflector that mimics a flat mirror for SPPs.[28] Similar ideas could be applied to the design of different devices, including the beam shifter analyzed in this work. Therefore, we are confident that the recipes that we have proposed could be practically implemented by properly structuring a dielectric layer placed on top of a metallic film at a length scale much smaller than the operating wavelength.

In conclusion, we have demonstrated how the concept of transformation optics when applied to SPP propagation could offer the necessary tools to design new strategies for molding the flow of SPPs in structured metal surfaces. A simplification of the general TO recipes in which only the dielectric side is manipulated yields to almost perfect functionalities for SPP devices. We hope that our results will encourage other experimental and theoretical groups to explore the exciting opportunities that the idea of transformation optics brings into the field of plasmonics.

Note: As we completed this paper, we discovered that another group[29] also completed a paper independently at the same time on a similar topic.

Acknowledgment. This work has been sponsored by the Spanish Ministry of Science under Projects MAT2009-06609-C02 and CSD2007-046-NanoLight. P.A.H. acknowledges financial support from the Spanish Ministry of Education through Grant AP2008-00021.

REFERENCES AND NOTES

(1) Pendry, J. B.; Schurig, D.; Smith, D. R. Controlling electromagnetic fields. *Science* **2006**, *312*, 1780–1782.
(2) Leonhardt, U. Optical conformal mapping. *Science* **2006**, *312*, 1777–1780.
(3) Ward, A. J.; Pendry, J. B. Refraction and geometry in Maxwell's equations. *J. Mod. Opt.* **1996**, *43*, 773–793, 4.
(4) Leonhardt, U.; Philbin, T. G. General relativity in electrical engineering. *New J. Phys.* **2006**, *8*, 247.
(5) Schurig, D.; Mock, J. J.; Justice, B. J.; Cummer, S. A.; Pendry, J. B.; Starr, A. F.; Smith, D. R. Metamaterial electromagnetic cloak at microwave frequencies. *Science* **2006**, *314*, 977–980.
(6) *Metamaterials: Physics and Engineering Explorations*; Ziolkowski, R. W., Engheta, N., Ed.; John Wiley & Sons, Inc.: Hoboken, NJ, June 2006.
(7) Ramakrishna, S. A. Physics of negative refractive index. *Rep. Prog. Phys.* **2005**, *68*, 449–521.
(8) Liu, R.; Ji, C.; Mock, J. J.; Chin, J. Y.; Cui, T. J.; Smith, D. R. Broadband ground-plane cloak. *Science* **2009**, *323*, 366–369.
(9) Valentine, J.; Li, J.; Zentgraf, T.; Bartal, G.; Zhang, X. An optical cloak made of dielectrics. *Nat. Mater.* **2009**, *8*, 568–571.
(10) Gabrielli, L. H.; Cardenas, J.; Pointras, C. B.; Lipson, M. Silicon nanostructure cloak operating at optical frequencies. *Nat. Photonics* **2009**, *43*, 461–463.
(11) Li, J.; Pendry, J. B. Hiding under the carpet: a new strategy for cloaking. *Phys. Rev. Lett.* **2008**, *101*, 203901.
(12) Rahm, M.; Cummer, S. A.; Schurig, D.; Pendry, J. B.; Smith, D. R. Optical design of reflectionless complex media by finite embedded coordinate transformations. *Phys. Rev. Lett.* **2008**, *100*, No. 063903.
(13) Rahm, M.; Schurig, D.; Roberts, D. A.; Cummer, S. A.; Smith, D. R.; Pendry, J. B. Design of electromagnetic cloaks and concentrators using form-invariant coordinate transformations of Maxwell's equations. *Photonics Nanostruct. Fundam. Appl.* **2008**, *6*, 87–95.
(14) Kildishev, A. V.; Shalaev, V. M. Engineering space for light via transformation optics. *Opt. Lett.* **2008**, *33*, 43–45.

DOI: 10.1021/nl100800c | *Nano Lett.* **2010,** *10,* 1985–1990

(15) Roberts, D. A.; Rahm, M.; Pendry, J. B.; Smith, D. R. Transformation-optical design of sharp waveguide bends and corners. *Appl. Phys. Lett.* **2008**, *93*, 251111.
(16) Schurig, D.; Pendry, J. B.; Smith, D. R. Transformation-designed optical elements. *Opt. Express* **2007**, *15*, 14772–14782.
(17) Han, S.; Xiong, Y.; Genov, D.; Liu, Z.; Bartal, G.; Zhang, X. Ray optics at a deep-subwavelength scale: a transformation optics approach. *Nano Lett.* **2008**, *8*, 4243–4247.
(18) Barnes, W. L.; Dereux, A.; Ebbesen, T. W. Surface plasmon subwavelength optics. *Nature* **2003**, *424*, 824–830.
(19) Maier, S. A.; Atwater, H. A. Plasmonics: localization and guiding of electromagnetic energy in metal/dielectric structures. *J. Appl. Phys.* **2005**, *98*, No. 011101.
(20) Bozhevolnyi, S. I.; Genet, C.; Ebbesen, T. W. Surface-plasmon circuitry. *Phys. Today* **2008**, (May), 44.
(21) Gramotnev, D. K.; Bozhevolnyi, S. I. Plasmonics beyond the diffraction limit. *Nat. Photonics* **2010**, *4*, 83.
(22) Ditlbacher, H.; Krenn, J. R.; Schider, G.; Leitner, A.; Aussenegg, F. R. Two-dimensional optics with surface plasmon polaritons. *Appl. Phys. Lett.* **2002**, *81*, 1762.
(23) Alù, A.; Engheta, N. Achieving transparency with plasmonic and metamaterial coatings. *Phys. Rev. E* **2005**, *72*, No. 016623.
(24) Baumeier, B.; Leskova, T. A.; Maradudin, A. A. Cloaking from surface plasmon polaritons by a circular array of point scatterers. *Phys. Rev. Lett.* **2009**, *103*, 246803.
(25) Smolyaninov, I. I.; Hung, Y. J.; Davis, C. C. Two-dimensional metamaterial structure exhibiting reduced visibility at 500 nm. *Opt. Lett.* **2008**, *33*, 1342–1344.
(26) Knupp, P. Steinberg, S., *Fundamentals of grid generation*; CRC Press: Boca Raton, FL, 1994.
(27) Cai, W.; Chettiar, U. K.; Kildishev, A. V.; Shalaev, V. M. Optical cloaking with metamaterials. *Nat. Photonics* **2007**, *1*, 224–227.
(28) Renger, J.; Kadic, M.; Dupont, G.; Aćimović, S.; Guenneau, S.; Quidant, R. Enoch, S., Hidden progress: broadband plasmonic invisibility, http://arxiv.org/ftp/arxiv/papers/1003/1003.5476.pdf.
(29) Liu, Y.; Zentgraf, T.; Bartal, G.; Zhang, X. *Nano Lett.* **2010**, DOI: 10.1021/nl1008019.

DOI: 10.1021/nl100800c | *Nano Lett.* **2010,** *10,* 1985--1990